

3  
4 **Determination of digoxin in serum samples using a flow flow-**  
5 **through fluorosensor based on a molecularly imprinted**  
6 **polymer**

7  
8 **Gema Paniagua González, Pilar Fernández Hernando\*, J. S. Durand Alegría**

9 *Departamento de Ciencias Analíticas, Facultad de Ciencias, Universidad Nacional de*  
10 *Educación a Distancia (UNED), 28040 Madrid (Spain).*

11  
12 \*Corresponding author. Phone: 0034(91)-3987284; Fax: 0034(91)-3988379. E-mail:  
13 [pfhernando@ccia.uned.es](mailto:pfhernando@ccia.uned.es).

14  
15  
16 **Abstract**

17 This work describes the development of a competitive flow-through FIA assay  
18 for digoxin using a molecularly imprinted polymer (MIP) as the recognition phase. In  
19 previous work, a number of non-covalent imprinted polymers were synthesised by  
20 “bulk” polymerisation. The digoxin binding and elution characteristics of these MIPs  
21 were then evaluated to obtain a highly selective material for integration into a sensor.  
22 The optimum MIP was synthesised by photo-initiated polymerisation of a mixture  
23 containing digoxin, MAA, EDGMA and AIBN in acetonitrile. The bulk polymer was  
24 ground and sieved and the template removed by soxhlet extraction in MeOH/ACN. The  
25 MIP was packed into a flow cell and placed in a spectrofluorimeter to integrate the  
26 reaction and detection systems. The physical and chemical variables involved in digoxin  
27 determination by the sensor (nature and concentration of solution, flow rates, etc.) were  
28 optimised. Binding with the non-imprinted polymer (NIP) was also analysed. The new  
29 fluorosensor showed high selectivity and sensitivity, a detection limit of  $1.7 \times 10^{-2} \mu\text{g L}^{-1}$ ,  
30 and high reproducibility (RSD of 1.03% and 1.77% for concentrations of  $1.0 \times 10^{-3} \mu\text{g L}^{-1}$   
31 and  $4.0 \times 10^{-3} \text{ mg L}^{-1}$  respectively). Selectivity was tested by determining the cross-

32 reactivity of several compounds with structures analogous to digoxin. Under the assay  
33 conditions used, in which the potential interfering compounds were in concentrations  
34 100 times higher than that of the analyte, no interference was recorded. The proposed  
35 fluorosensor was successfully used to determine digoxin concentration of human serum  
36 samples.

37

38 *Keywords:* Digoxin; Molecular imprinting; Fluorosensor; Human serum analysis

39

## 40 **1. Introduction**

41 The use of molecular imprinting in the design of new drug delivery systems and  
42 devices has attracted much attention in recent years. Molecularly imprinted polymers  
43 (MIPs) combine highly selective molecular recognition properties (comparable to those  
44 of biological systems) with characteristics such as physical robustness and good  
45 thermal, chemical and mechanical stability. This renders them particularly suitable for  
46 use as recognition elements in sensor technology (D'Agostino et al., 2006; Huang et al.,  
47 2007). Further, these materials can be employed in aqueous and non-aqueous media and  
48 can be manufactured in different configurations (e.g., as blocks, beads, microspheres,  
49 thin-films, filaments or microstructures) to facilitate their integration into sensor design  
50 (Lakshmi et al., 2006; Breton et al., 2006). MIPs can also be used in chromatographic  
51 separation (Watabe et. al., 2005), as selective adsorbents for cleaning samples (Chapuis  
52 et. al., 2006), in solid-phase extraction (Hu et. al., 2005; Baggiani et. al., 2007), and as  
53 catalysts (Vokmann and Brüggermann, 2006). Molecular imprinting is now an  
54 established technique for the production of molecular recognition materials with  
55 predetermined affinities for analytes such as amino acids (Li and Husson, 2006),  
56 proteins (Bossi et. al., 2007), carbohydrates (Furqan and Hansen, 2007), drug

57 compounds (Suede et. al., 2006), pesticides (Wei et. al., 2006), steroids, corticosteroids  
58 (Sun et. al., 2006), and metal ions (Kidschy and Alocilja, 2005).

59         Digoxin is a glycoside used in the treatment of congestive heart failure; in fact it  
60 has been used for this for over 200 years and is still one of the most widely prescribed  
61 heart failure drugs. Strict control of digoxin therapy is necessary, however, since there is  
62 a thin line separating therapeutic and toxic levels ( $0.05\text{-}0.2 \mu\text{g l}^{-1}$ ); sensitive and  
63 selective detection techniques are therefore required. This paper describes a flow-  
64 injection optical sensor for digoxin that combines sensor technology with a new  
65 generation of molecularly imprinted synthetic receptors. Preliminary work on the  
66 composition and synthesis conditions of this MIP has been reported (Paniagua et. al.,  
67 2006); this allowed the most suitable MIP for the new fluorosensor for digoxin to be  
68 chosen. MIPs were synthesised under different conditions, i.e., changing the functional  
69 monomer employed (methacrylic acid or 2-vinylpyridine) as well as the porogen  
70 (acetonitrile or dichloromethane). The polymerisation process was studied under UV  
71 light (365 nm) or in a thermostat-controlled waterbath (60°C) for 8 to 14 h. The binding  
72 and elution solutions, the concentration of the labelled antigen solution and the flow rate  
73 were all optimised. The binding of digoxin to the non-imprinted polymer (NIP) was  
74 also examined under optimum conditions. The proposed fluorosensor was highly  
75 selective and sensitive and provided highly reproducible results. The proposed  
76 fluorosensor was successfully used to determine the digoxin concentration of human  
77 serum samples.

78

79

80

81

## 82 **2. Material and Methods**

### 83 *2.1. Reagents*

84 Ethylene glycol dimethacrylate (EDMA) and methacrylic acid (MAA) were  
85 purchased from Merck (Darmstadt, Germany), 2-2'-azobisisobutyronitrile (AIBN) from  
86 Fluka (Buchs, Switzerland), and digoxin (95%), morphine, heroine, codeine, tebaine,  
87 pentazocine and narcotine from Sigma Aldrich (Madrid, Spain). Digoxin labelled with  
88 fluorescein isothiocyanate (FITC) ( $10 \mu\text{mol l}^{-1}$ ) was obtained from MicroPharm  
89 (Newcastle, Carmarthenshire, UK). Acetonitrile (ACN) and methanol (HPLC grade)  
90 were supplied by Scharlau (Barcelona, Spain). Phosphate buffer solution (PBS, pH=7.5)  
91 (NaCl 0.1 mM;  $\text{KH}_2\text{PO}_4$  1.4 mM; KCl 2.7 mM;  $\text{NaH}_2\text{PO}_4$  8 mM;  $\text{MgCl}_2$  21.3 mM),  
92 anhydrous sodium carbonate and sodium dodecylsulphate (SDS) were obtained from  
93 Merck (Darmstadt, Germany). Deionised water ( $18.3 \text{ M}\Omega \text{ cm}$ ) used in the preparation  
94 of aqueous solutions was obtained using a Milli-Q water system (Millipore Ibérica,  
95 Madrid, Spain).

96

### 97 *2.2. Instrumentation*

98 Fluorescence intensity was measured with a Perkin-Elmer LS-5  
99 spectrofluorimeter equipped with a 100  $\mu\text{l}$  Hellma (Jamaica, NY, USA) flow cell  
100 (optical path 3 mm) in conjunction with an AAT computer. The flow-injection system  
101 consisted of a Gilson Minipulse-2 peristaltic pump and an Omnifit six-way injection  
102 valve. PTF tubes (0.5 mm i.d) were used to build the manifold. The pH was measured  
103 using a Metrohm 654 pH meter. An ultraviolet lamp (Vilber Lourmat CN-6T) was used  
104 to induce polymerisation. The morphology of the polymer was characterised using a  
105 Jeol JSM-6400 scanning electron microscope (SEM). The surface area of the imprinted

106 polymer was characterized using a Micromeritics ASAP 2000 apparatus (Norcross,  
107 USA).

108

### 109 *2.3. Procedures*

#### 110 *Preparation of the molecularly imprinted polymer*

111 In preliminary work (Paniagua et. al., 2006), a number of polymers were  
112 prepared by bulk polymerisation under different synthesis conditions in order to select  
113 that with the best digoxin-recognition characteristics. Several functional monomers  
114 (methacrylic acid or 2-vinylpyridine) and different types of porogen (ACN, chloroform  
115 or dichloromethane) were tested. The best polymerisation procedure (either employing  
116 a UV source or a thermostat-controlled waterbath) and extraction process (soxhlet or  
117 microwave extraction) were also determined. The surface morphology of the polymers  
118 was analysed by SEM, and the binding affinity of the different digoxin-MIPs evaluated  
119 by equilibrium binding experiments. The molecular ratio of the optimum polymer was  
120 ( $10^{-3}$ :1:5) digoxin:MAA:EDMA. The fluorosensor was equipped with this polymer,  
121 which was prepared in a glass tube by the bulk polymerisation method using a mixture  
122 of the template molecule ( $2.0 \times 10^{-3}$  mmol), methacrylic acid (2.0 mmol), ethylene glycol  
123 dimethacrylate (10.0 mmol), 2-2'-azobisisobutyronitrile ( $6.0 \times 10^{-2}$  mmol), and 10 ml of  
124 ACN as a porogen. The pre-polymerisation mixture was degassed with nitrogen for 5-  
125 10 min. A control polymer were prepared using the same composition but in the  
126 absence of the template. The glass tube was then exposed to the UV source ( $\lambda$ /nm 365  
127 nm) at 10°C for 24 h. After polymerisation, the polymer block was removed from the  
128 glass tube and was manually ground in a mortar and sieved to a particle size of 355-600  
129  $\mu$ m. The template was extracted by the Soxhlet system with MeOH:ACN (50:50, v/v)  
130 over a period of 20 h.

131 *Preparation of the fluorosensor*

132 Figure 1 shows the fluorosensor apparatus. The reactor was a flow-through cell  
133 (100  $\mu\text{l}$ ) packed with the sensitive phase (digoxin-MIP); this was placed in the  
134 spectrofluorimeter, thus integrating the reaction and detection systems. The flow stream  
135 was generated by an upstream peristaltic pump. The samples were introduced into the  
136 system by a six-way valve equipped with a 150  $\mu\text{l}$  sample loop.

137

138 *Sample preparation*

139 Digoxin-containing serum samples were supplied by the Puerta de Hierro  
140 Hospital (Madrid). These were stored at 4°C. Sample aliquots of 650  $\mu\text{l}$  were added to  
141 900  $\mu\text{l}$  of ACN and centrifuged at 3500 rpm for 30 min to precipitate the proteins.

142 *Competitive assay protocol for the determination of digoxin in serum samples*

143 To determine the digoxin concentration of the serum samples, a heterogeneous  
144 fluorescent competitive assay was undertaken in which the digoxin competed with a  
145 fluorescent tracer (FITC-digoxin) for recognition sites in the digoxin-MIP. For this,  
146 1700  $\mu\text{l}$  of purified serum was mixed with 170  $\mu\text{l}$  of FITC-digoxin (0.2  $\mu\text{mol l}^{-1}$ ). The  
147 competitive calibration curve was obtained using digoxin solutions (1000  $\mu\text{l}$ ) at  
148 different concentrations (0-4 $\times 10^{-3}$  mg  $\text{l}^{-1}$ ) in ACN. This required a digoxin stock  
149 solution (0.5 ppm) be prepared in a mixture of ACN and  $\text{Na}_2\text{CO}_3$  (0.1 M, pH=8.0)  
150 (50:50 v/v). For the preparation of the standard solutions, different aliquots of the 0.5  
151 stock solution were added to 100  $\mu\text{l}$  of FITC-digoxin (1:50 in ACN, 0.2  $\mu\text{mol l}^{-1}$ ), and  
152 ACN then added to 1000  $\mu\text{l}$ . 150  $\mu\text{l}$  of corresponding standard were then injected into  
153 the carrier solution (ACN) at a flow rate of 0.27  $\text{ml min}^{-1}$ . Excess antigens, labelled and  
154 unlabelled, were removed by the carrier solution. The fluorescence signal generated was

155 measured *in situ* in the reactor at  $\lambda_{em}/nm$  517 and  $\lambda_{exc}/nm$  496. Finally, an elution  
156 solution (MeOH/ACN, 90:10) was pumped into the flow cell to regenerate the reactor.

157

### 158 **3. Results and Discussion**

#### 159 *3.1. Optimisation of experimental conditions and characterisation of the sensor*

160 The sensitivity, selectivity and response time of the fluorescent sensor were  
161 determined. The composition of the polymer and its polymerisation conditions were  
162 determined in previous work (Paniagua et. al., 2006). The greatest specific binding was  
163 achieved with ACN (42%). This solvent showed a very low binding affinity for the  
164 control polymer; non-specific binding was 19%. The percentage uptake with the  
165 imprinted polymer was 61%. Using this information it was possible to select the  
166 polymer best suited to act as the recognition phase in the proposed sensor.

167 The effect of polymerisation on the particle structure of the methacrylic polymer  
168 was also examined. The surface area, specific pore volume and average pore diameter  
169 of the polymer were obtained by nitrogen sorption porosimetry. The MIP had a specific  
170 surface area of  $31.844\text{ m}^2\text{ g}^{-1}$  and a specific pore volume of  $0.194\text{ cm}^3\text{ g}^{-1}$ . The pore size  
171 distribution was macropores 50%, mesopores 44.33%, and micropores 5.67%.

172 The study of the binding mechanism and regeneration of the polymer was  
173 carried out. The efficacy of the retention process was affected by the carrier solvent, pH,  
174 and the flow rate. The amount of labelled digoxin used was optimised in order to obtain  
175 good sensitivity and a strong fluorescence signal. For this, 150  $\mu\text{l}$  of digoxin-FITC at  
176 different concentrations (0.0075; 0.15; 0.2; 0.3  $\mu\text{mol l}^{-1}$ ) plus several carrier solvents  
177 (ACN, MeOH and aqueous phosphate buffer solution PBS, pH=7.5) were assayed by  
178 spectrofluorimetry at  $\lambda_{exc}/nm$  496 ( $\lambda_{em}/nm$  517). Figure 2 shows the fluorescence  
179 signals obtained using different binding solutions for different concentrations of FITC-

180 digoxin. The effect of the binding solution flow rate was studied in the range 0.1 to 0.6  
181 ml min<sup>-1</sup>. The effect of pH (3-9) was also tested. ACN at pH 9.0 was finally selected as  
182 the carrier solution. The optimum flow rate was 0.27 mL min<sup>-1</sup>. With a slightly higher  
183 flow rate (0.3 ml min<sup>-1</sup>) no improvements were seen; higher flow rates considerably  
184 reduced the retention of the polymer. To increase the strength of the fluorescence  
185 signals, the tensactive effect of different concentrations (4.0, 6.0, 8.0 and 10.0 mM) of  
186 SDS was examined; 100 µl SDS of each concentration were added to 50 ml of ACN.  
187 The best fluorosensor response was obtained when working close to the critical micellar  
188 concentration (8.1 mM) of SDS; the optimum value was 8.0 mM.

189 To prevent the polymer losing binding capacity, the optimum washing time was  
190 determined, and regeneration solutions used to regenerate the reactive phase. The effect  
191 of a 30-120 s washing time was studied for a 0.2 µmol l<sup>-1</sup> digoxin-FITC solution; the  
192 optimum time was 80 s. Shorter times did not allow the polymer to regenerate, thus  
193 reducing its binding capacity. Longer times did not improve the process. MeOH:H<sub>2</sub>O  
194 (70:30, 50:50 and 30:70), MeOH:ACN (90:10), MeOH:ACN:H<sub>2</sub>O (80:10:10) and  
195 MeOH and H<sub>2</sub>O were all tested as regeneration solutions. Figure 3 shows their elution.  
196 MeOH:ACN (90:10) provided the best results.

197 A binding assay using NIP as the reactive phase was undertaken under optimum  
198 conditions. No digoxin bound to the NIP.

199

### 200 3.2. Analytical performance

201 To determinate the selectivity of the MIP, cross-reactivity with narcotine,  
202 tebaine, heroine, pentazocine, morphine and codeine was examined. For interference  
203 studies, competitive calibration curves were plotted, using concentrations of 0-6×10<sup>2</sup> µg  
204 l<sup>-1</sup> of digoxin. The ratios between the I<sub>50</sub> values determined for digoxin and the

205 potentially interfering substances were calculated. In no case was cross reactivity  
206 detected, even when the concentration of the test molecules was 100 times that of the  
207 analyte (Fig. 5).

208 A competitive calibration curve was obtained for the working range of  $0-4 \times 10^{-3}$   
209  $\text{mg l}^{-1}$  digoxin and  $0.2 \mu\text{mol l}^{-1}$  of FITC-digoxin. The normalized fluorescence signal,  
210 %B/Bo (where B is the intensity of fluorescence of the conjugated digoxin at different  
211 standard concentrations of digoxin, and Bo that of the blank), was plotted against the  
212 digoxin concentration. Figure 4 shows the calibration curve obtained. The curve  
213 equation was:  $\%B/Bo = 9 \times 10^6 C^2 - 5 \times 10^4 C + 96$  ( $n=5$ ,  $r=0.990$ ). The detection limit (X-  
214 2SD) was calculated using five replicates of zero standards and expressed as the least  
215 detectable dose (LDD) of digoxin; under optimum conditions this was  $1.7 \times 10^{-2} \mu\text{g l}^{-1}$ .  
216 The relative standard deviations (RSD) of six determinations for  $1 \times 10^{-3}$  and  $4 \times 10^{-3} \text{mg l}^{-1}$   
217 digoxin were 1.0% and 1.8% respectively; for the serum samples an RSD of <10% was  
218 obtained. The total time required for each assay was 400 s. The lifetime of the sensor  
219 without loss of sensitivity was approximately 18 months; no special storage conditions  
220 were necessary to maintain optimum performance.

221

### 222 3.3. Sample analysis application

223 Table 1 shows the results of the determination of digoxin in the serum samples  
224 obtained using the proposed method and a reference method (MEIA, microparticle  
225 immunoenzyme assay, Abbott Laboratories). No significant differences were seen  
226 between the values obtained ( $p < 0.05$ ).

227

228

229

230 **4. Conclusions**

231 This paper proposes a new molecularly imprinted fluorescence sensor for  
232 determining the concentration of digoxin in serum. Strategies for selecting the best  
233 combination of monomers, cross-linkers, solvents and polymerisation conditions for  
234 production of the MIP were established. This included determining the best morphology  
235 of the MIP and the optimum pore size. The polymer finally chosen showed good  
236 digoxin-recognition properties and was sufficiently stable for integration into a flow-  
237 through fluorosensor. The imprinted polymer showed good thermal (up to 80°C) and  
238 chemical stabilities and can be used over the pH range 3-9; no digoxin bound to the  
239 NIP. Cross-reactivity with compounds of similar structures was negligible.  
240 Consequently, this fluorosensor is highly sensitive and selective for digoxin. The  
241 analysis and regeneration time is very short (about 400 s). When used to determine  
242 digoxin concentrations in human serum, the fluorosensor provided satisfactory results.

243

244 **Acknowledgements**

245 The authors thank the Spanish Ministry of Science and Technology for financial  
246 support (project CTQ 2006 -15027/PPQ), the Puerta de Hierro Hospital for supplying  
247 serum samples and Adrian Burton for correcting the manuscript.

248

249 **References**

- 250 Baggiani, C., Baravalle, P., Giraudi, G., Tozzi, C., 2007. *J. Chromatog. A* 1141, 158-  
251 164.
- 252 Bossi, A., Borini, F., Turner, A.P.F., Pilektski, S.A., 2007. *Biosens. Bioelectron.* 22,  
253 1131-1137.
- 254 Breton, F., Euzet, P., Piletski, S.A., Giardi, M.T., Rouillon, R., 2006. *Anal. Chim. Acta*  
255 569, 50-57.
- 256 Chapuis, F., Mullot, J.U., Pichón, V., Tufall, G., Jennion, M.C., 2006. *J. Chromatog. A*  
257 1135, 127-134.
- 258 D'Agostino, G., Alberti, G., Biesuz, R., Pesavento, M., 2006. *Biosens. Bioelectron.* 22,  
259 145-152.
- 260 Furqan, M. F., Hansen, D.E., 2007. *Biorg. Medic. Chem. Lett.* 17, 235-238.
- 261 Huang, C.Y., Syu, H.J., Chang, Y.S., Chuan, T., Liu, B.D., 2007. *Biosens. Bioelectron.*  
262 22, 1694-1699.
- 263 Hu, S.G., Li, L., He, X.W., 2005. *J. Chromatog. A* 1062, 31-37.
- 264 Kidschy, L.M., Alocilja, E.C., 2005. *Biosens. Bioelectron.* 20, 2163-2167.
- 265 Lakshmi, D., Prasad, B. ., Sharma, P.S.S., 2006. *Talanta* 70, 272-280.
- 266 Li, X., Husson, S.M., 2006. *Biosens. Bioelectron.* 22, 336-348.
- 267 Paniagua, G., Fernández, P., Durand, J.S., 2006. *Anal. Chim. Acta* 557, 179-183.
- 268 Suede, R., Seechamnaturakit, V., Canyuk, B., Ovatalarnporn, C., Martin, G. P., 2006.  
269 *J. Chromatogr. A* 1114, 239-249.
- 270 Sun, H.W., Qiao, F.X., Liu, G.Y., 2006. *J. Chromatogr. A* 1134, 194-200.
- 271 Vokmann, A., Brüggermann, O., 2006. *React. Funct. Polym.* 66, 1725-1733.
- 272 Watabe, Y., Hosoya, H., Tanaka, N., Kerbo, Y., Kondo, T., Morita, M., 2005. *J.*  
273 *Chromatogr. A* 1073, 363-370.

274 Wei, S., Molinelli A., Mizaikoff. B., 2006. Biosen. Bioelectron. 21, 1943-1951.

275

276

277

278 **FIGURE LEGENDS**

279

280 Fig. 1. The flow-through sensor system.

281

282 Fig. 2. Binding studies on MIP for different concentrations of digoxin-FITC and  
283 solvents. Carrier solutions: ACN, MeOH, PBS (10 mM, pH= 7.5). Flow rate: 0.27 ml  
284 min<sup>-1</sup>. Digoxin-FITC concentrations ( $7.5 \times 10^{-3}$ ; 0.15; 0.2; 0.3  $\mu\text{mol l}^{-1}$ ).

285

286 Fig .3. Elution percentages for different solutions. Carrier solution: ACN (pH= 9; SDS  
287 8mM). Flow rate: 0.27 ml min<sup>-1</sup>, [digoxin-FITC]= 0.2  $\mu\text{mol l}^{-1}$ .

288

289 Fig. 4. Calibration curve for the optimum sensor, obtained by plotting the normalized  
290 signal against the digoxin concentration.

291

292 Fig. 5. Calibration curves obtained with the optimum fluorosensor for digoxin and  
293 structurally analogous compounds.

294

295 **TABLES**

296 Table 1

297 Results of human serum samples analysis

---

	Fluorosensor	Reference method
Sample	$10^{-4} (X \pm SD)/\text{ng } \mu\text{l}^{-1}$	$10^{-4} (X \pm SD)/\text{ng } \mu\text{l}^{-1}$
1	$(7.6 \pm 0.8)$	$(8.0 \pm 0.3)$
2	$(2.5 \pm 0.2)$	$(3.0 \pm 0.2)$
3	$(21.0 \pm 2.1)$	$(24.2 \pm 1.3)$
4	$(9.1 \pm 0.6)$	$(9.0 \pm 0.3)$
5	$(15.2 \pm 0.9)$	$(19.0 \pm 2.1)$
6	$(8.4 \pm 0.7)$	$(8.0 \pm 0.4)$

---

298

299

300 **FIGURES:**

301

302

303

304

305

306

307

308

309

310

311

312

313

314

315

316

317

318

319

320

321

322

323

324

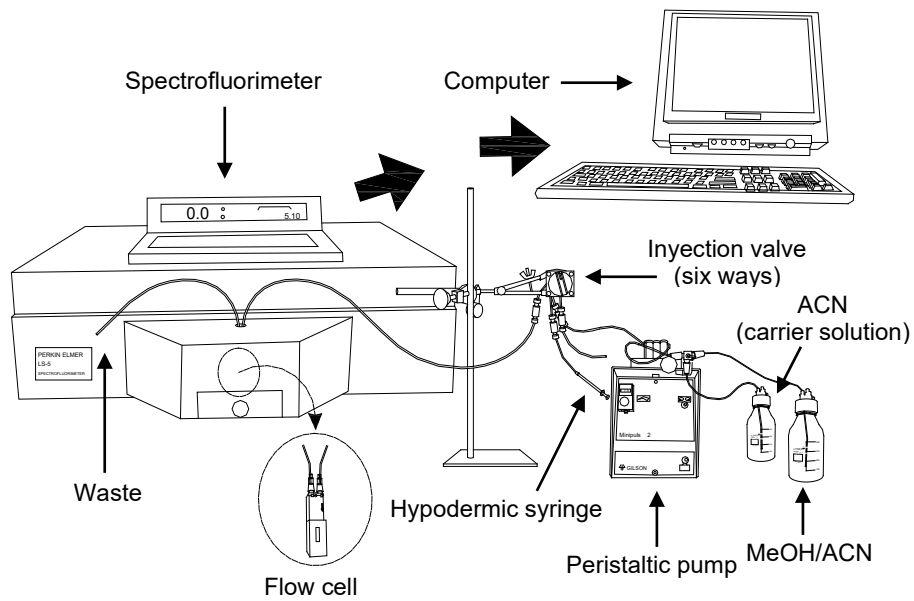


Fig.1

325

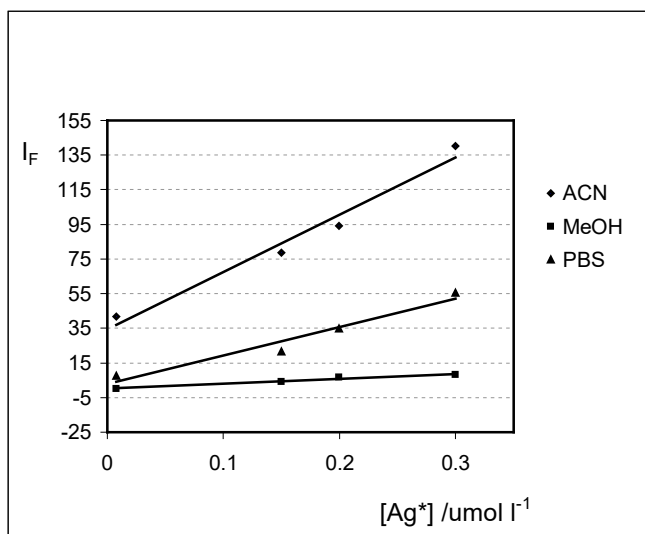


Fig.2

326

327

328

329

330

331

332

333

334

335

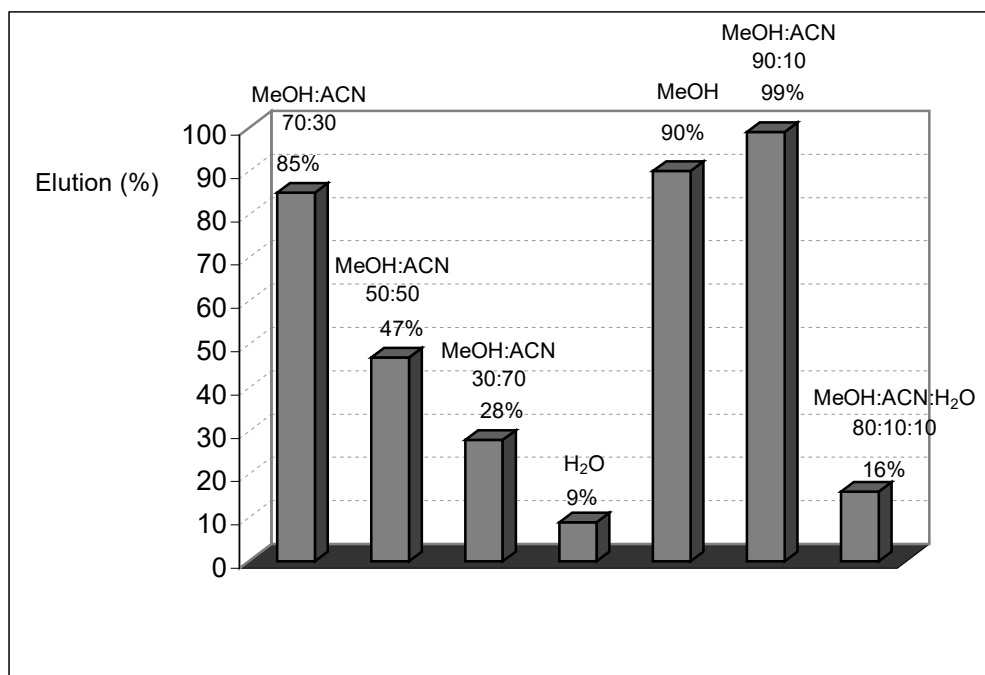
336

337

338

339

340



341  
342  
343

Fig.3

344  
345  
346  
347  
348  
349  
350  
351  
352  
353  
354  
355  
356  
357  
358  
359  
360  
361  
362  
363  
364  
365  
366  
367

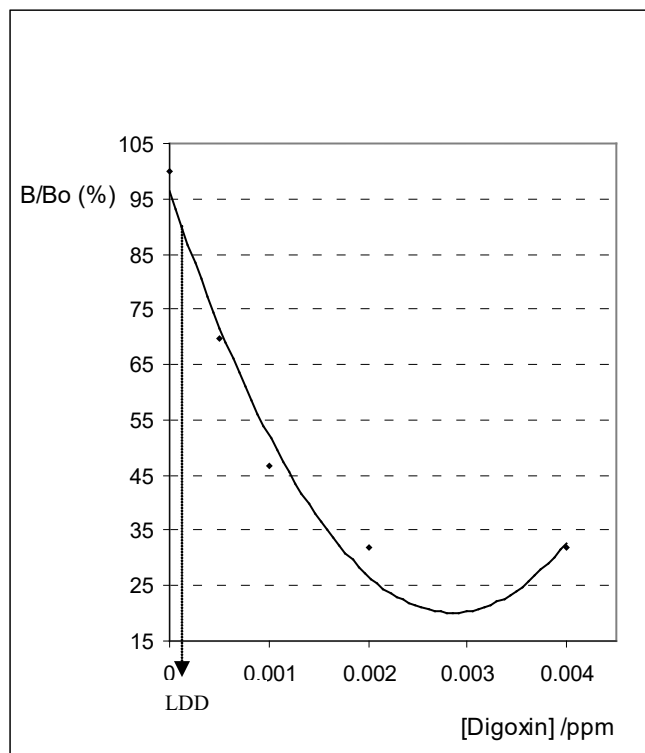


Fig.4

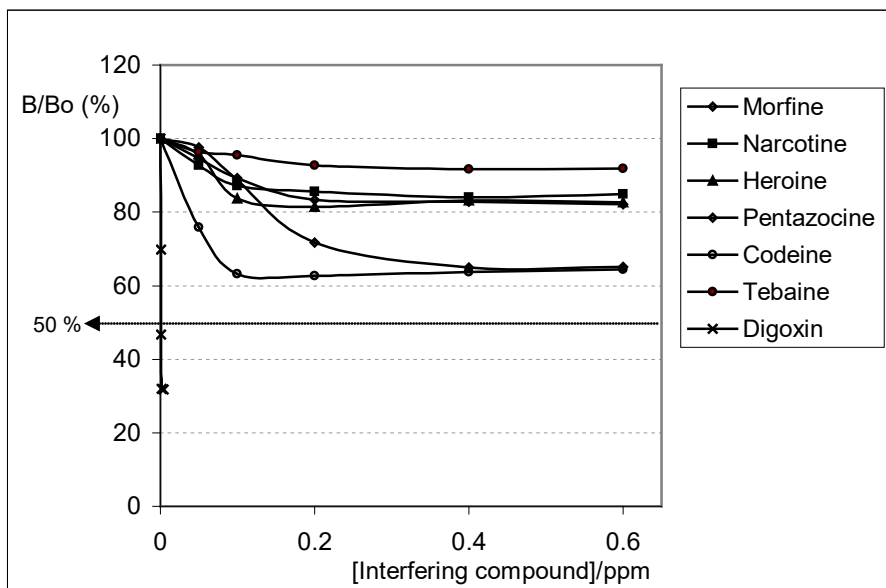


Fig. 5

368

369

370

371

372

373

374

375

376

377

378

379

380

381

382